# Supporting Information

# Synchrotron-Based Infrared Microanalysis of Biological Redox Processes under Electrochemical Control

Philip A. Ash,[†] Holly A. Reeve,[†] Jonathan Quinson,[†] Ricardo Hidalgo,[†] Tianze Zhu,[†] Ian J. McPherson,[†] Min-Wen Chung,[†] Adam J. Healy,[†] Simantini Nayak,[†] Thomas H. Lonsdale,[†] Katia Wehbe,[‡] Chris S. Kelley,[‡] Mark D. Frogley,[‡] Gianfelice Cinque,*[,‡] Kylie A. Vincent*[,†]

[†]Inorganic Chemistry Laboratory, Department of Chemistry, University of Oxford, South Parks Road, Oxford, Oxfordshire OX1 3QR, United Kingdom

[‡]Diamond Light Source, Harwell Science and Innovation Campus, Didcot, Oxfordshire OX11 0QX, United Kingdom

## Contents

## S1. Preparation of cell-free extract of NuoF subunit of *E. coli* complex I

### NuoF expression strain

The *nuoF* genes from *nuo* operon in *E. coli* genome were amplified by PCR using PCR Hot Start (Merck) and primers 5'-CATGCCATGGAAAACATTATCCGTACTCCC-3' and 5'-CCGCTCGAGCCAGCGCTCTTTCAG CAGGTT-3' (EuroFins Genomics). PCR reactions consisted of 1X KOD Hot Start Polymerase buffer, 2 mM $MgSO_4$, 0.2 mM (each) deoxynucleoside triphosphates (dNTPs), DMSO (4 %), 0.02 U $uL^{-1}$ KOD Hot Start polymerase (Novagen), 1 ng $uL^{-1}$ template DNA and 0.06 mM of both forward and reverse primers. PCR was carried out as follows: initial denaturation step (95 $^{o}$C, 3 min), followed by 30 cycles of denaturation at 94 $^{o}$C (30 s), annealing at 68 $^{o}$C (60 s) and elongation at 70 $^{o}$C (210 s) with a final extension at 70 $^{o}$C (10 min).

The template DNA and PCR fragment were digested with endonuclease NcoI and XhoI (NEB) and the PCR product was purified using QIAquick PCR purification kit (QIAGEN). The *nuoF* fragment was inserted into pET28a vector using T4 DNA ligase (NEB, 20 U $uL^{-1}$) for inclusion of a 6x Histag at the 3' end of the *nuoF* gene. The resulting plasmid (pETnuoF) was transformed into *E. coli* DH5α competent cells (Merck). Single colonies were selected and grown overnight at 37 $^{o}$C (10 mL LB medium, 50 μg $mL^{-1}$ kanamycin). The plasmid was isolated (QIAquick PCR purification kit, QIAGEN) and confirmed by sequencing (Science BioSource). Finally, the pETnuoF plasmid was transformed into *E. coli* BL21 DE3 competent cells (Merck) for over expression.

### Preparation of NuoF cell-free extract

The *E. coli* cells containing pETnuoF (1 mL) were grown in LB medium (600 mL, 37 $^{o}$C, 120 rpm) until an optical density of 0.6 at 600 nm was reached. The temperature was then lowered to 16 $^{o}$C for 1 hour before addition of IPTG (10 μM), FMN (20 μg $ml^{-1}$), sodium sulfate (2 μg $ml^{-1}$) and ferric ammonium citrate (100 μg $mL^{-1}$) to induce expression of NuoF overnight. The cells were harvested by centrifugation (4000 × *g*, 4 $^{o}$C, 30 min). The cells were resuspended in 50 mM MES buffer pH 6 (100 mM NaCl, 10% glycerol, 0.1% Triton X100) before lysing by sonication (15 s pulses/pause for 5 min). The cell debris was removed by centrifugation (10000 × *g*, 4 $^{o}$C, 30 min), and the cell-free extract (CE) containing NuoF was concentrated 10-fold (30 kDa Vivaspin, GE healthcare, 4000 × *g*, 30 min). Presence of the NuoF protein was confirmed by SDS-PAGE (Figure S1(A)). Colorimetric assays confirming that the NuoF is active are shown in Figure S1(B).

**Preparation of NuoF-deficient cell-free extract as control 'dummy' cells**

The *nuoE* genes from *nuo* operon in *E. coli* genome were amplified by PCR using PCR Hot Start (Merck) and primers 5'-GCGTCGACTTTATACCGCTCCAGCAG-3' and 5'-CCGCTCGAGCCAGCGCTCTTTCAG CAGGTT-3' (EuroFins Genomics). Due to the stop code upstream of the NuoF genes, these cells produced only NuoE. Cell-free extract of these NuoF-deficient 'dummy' cells were prepared in the same way as described above for NuoF. NuoE is an electron transport subunit of Complex 1 and contains 1 FeS cluster but does not contain a Flavin center.

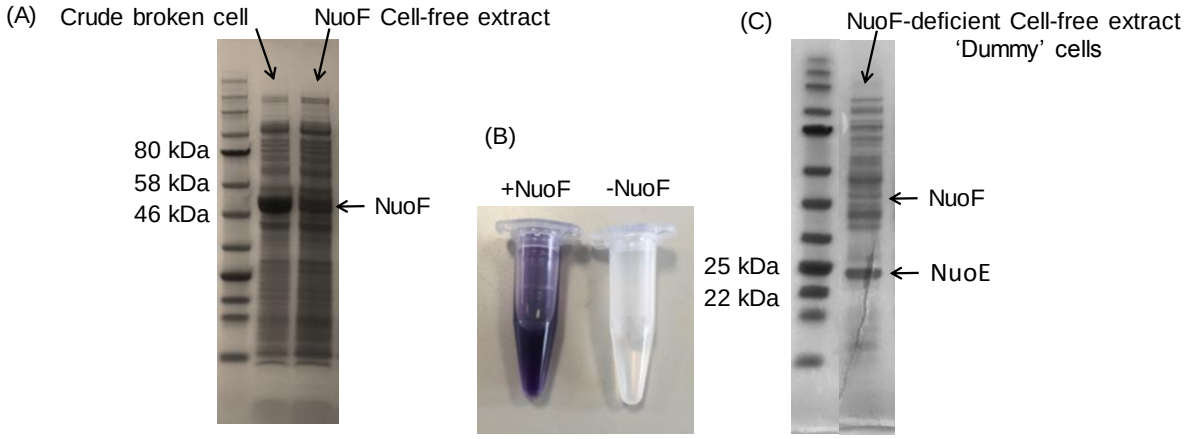


**Figure S1:** (A) SDS-PAGE gel showing over expression of NuoF in whole broken cells and the cell-free extract after removal of the cell debris. NuoF represents *ca* 50 % of the total protein. (B) Cell-free extract from BL21 DE3 cells with (+NuoF) and without (-NuoF) over expression of *nuoF* genes were analyzed using a benzyl viologen colorimetric test. Reactions contained NADH (4 mM), benzyl viologen (4 mM) and cell-free extract (20 µL) in 50 mM MES buffer (pH 6, 1 mL). The reactions were incubated at 37 $^{o}$C for 10 minutes and initiated by addition of an aliquot of the specified cell-free extract. Development of a purple color demonstrates benzyl viologen reduction. Assays were performed in the presence and absence of NADH and only those containing NuoF and NADH led to reduction of benzyl viologen. This demonstrates that the NuoF is active and that only NuoF is contributing to benzyl viologen mediated NADH oxidation activity. (C) SDS-PAGE gel showing expression of NuoE and no significant generation of NuoF in the 'Dummy' cells

**Figure S2.** Scale diagram showing the size and position of electrodes and solution flow inlet/outlet within the microspectroscopy cell. RE: reference electrode; WE: working electrode; AE: counter (auxiliary) electrode.

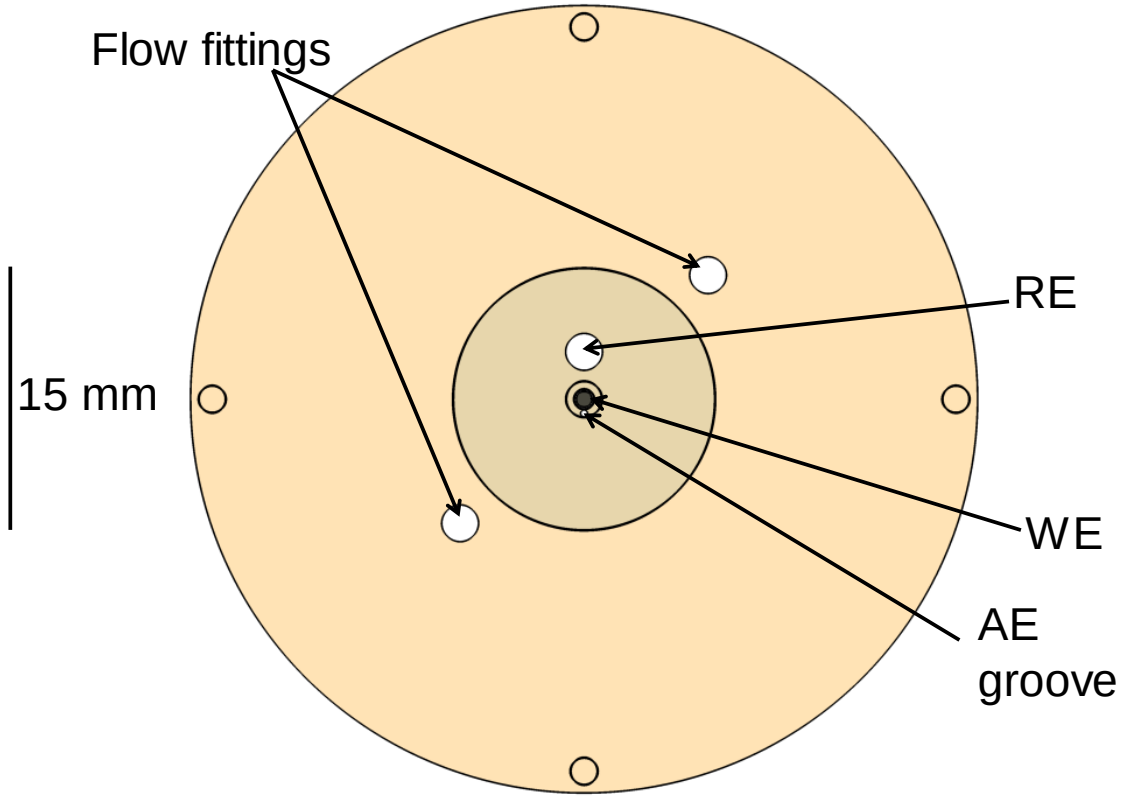

**Figure S3.** Comparison of the electrochemical responses of the microspectroscopy and ATR-IR spectroelectrochemical cells used in this work.

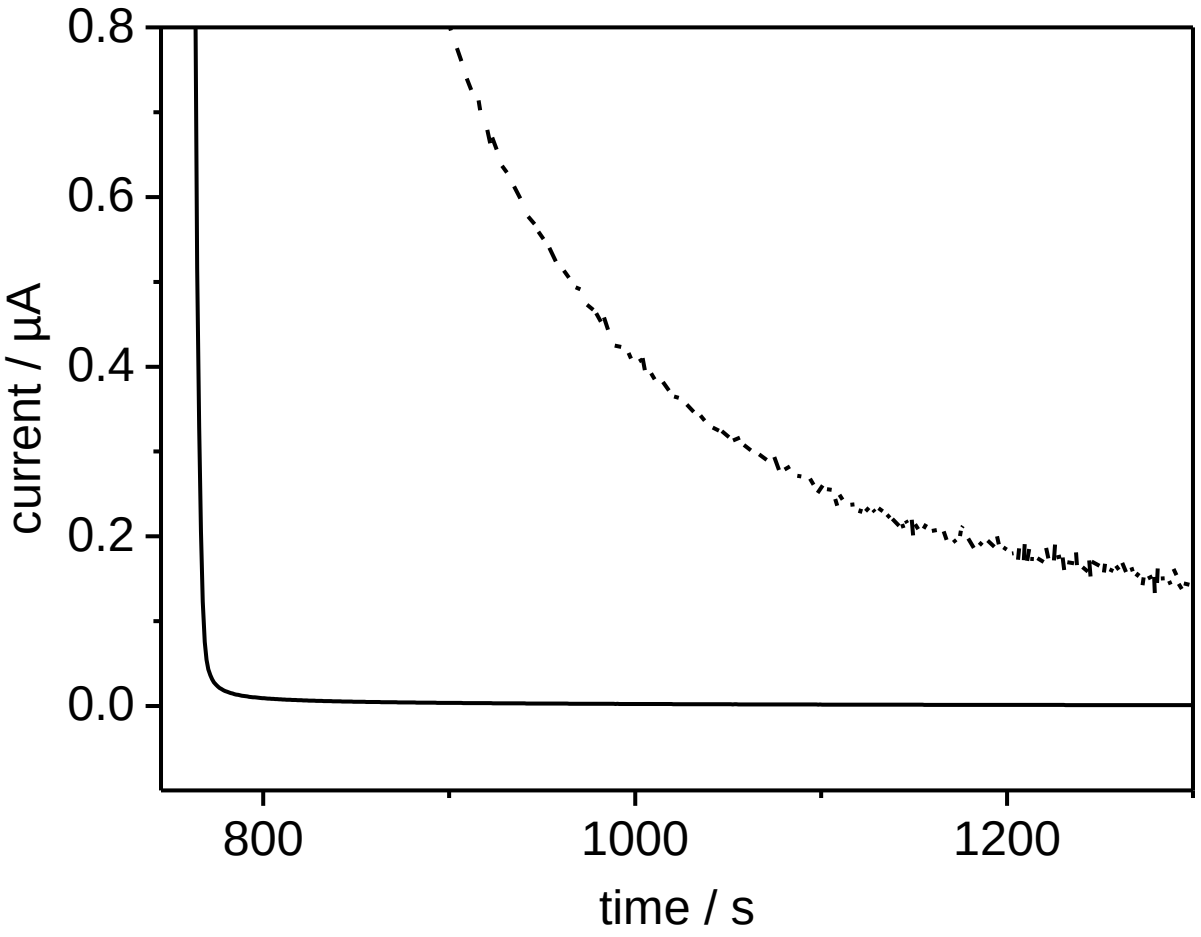


Electrochemistry of FMN adsorbed on carbon black particles. Current-time trace following a potential step from -0.558 V to +0.242 V in the ATR-IR (dashed) and reflection-absorption microspectroscopy (solid) cells. Data are reproduced from the third applied potential in Figure 2 of the main text; the time axis directly correlates between both figures. Potassium phosphate buffer, pH 6, containing 100 mM KCl was used as background electrolyte.

**Figure S4.** Typical particle-modified electrode used in the microspectroscopy cell.

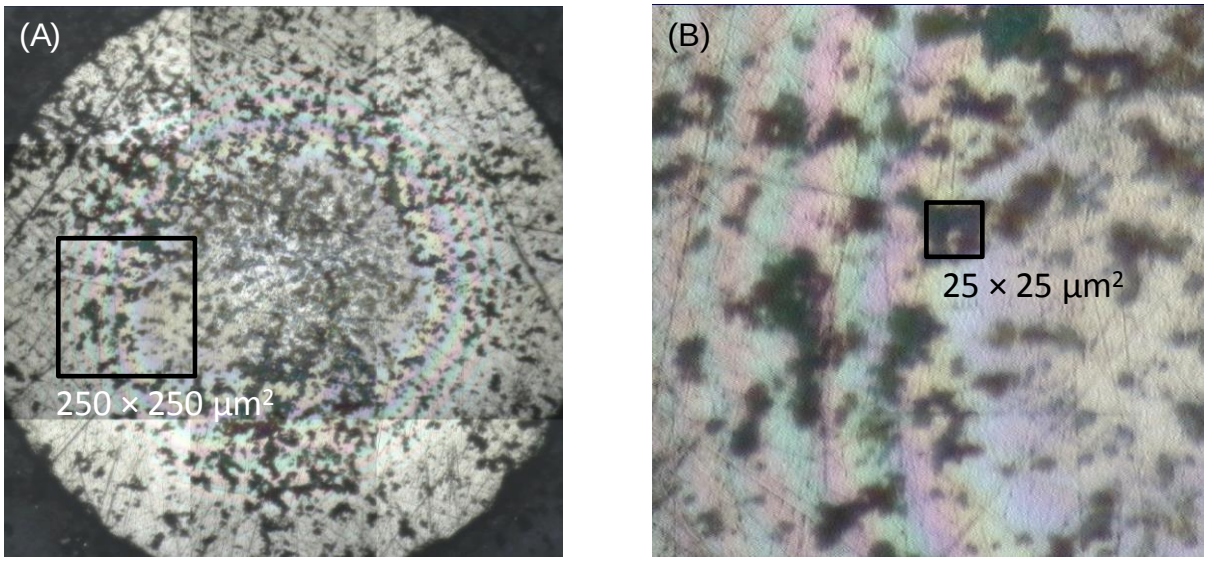


(A) Visible image of the particle-modified electrode used to record the NuoF CE difference spectrum shown in Figure 4 of the main text. Carbon black particles (Black Pearls 2000, Cabot corp.), pretreated with NuoF CE, were drop cast onto the electrode before assembly of the microspectroscopy cell. Image collected using a 15× objective. (B) Expanded view of the square region indicated in (A), showing the 25 × 25 $\mu m^2$ area containing the particle aggregate from which the difference spectrum in Figure 4 of the main text was calculated. Image collected using a 36× objective.

**Figure S5.** Baseline noise level of the miscrospectroscopy cell.

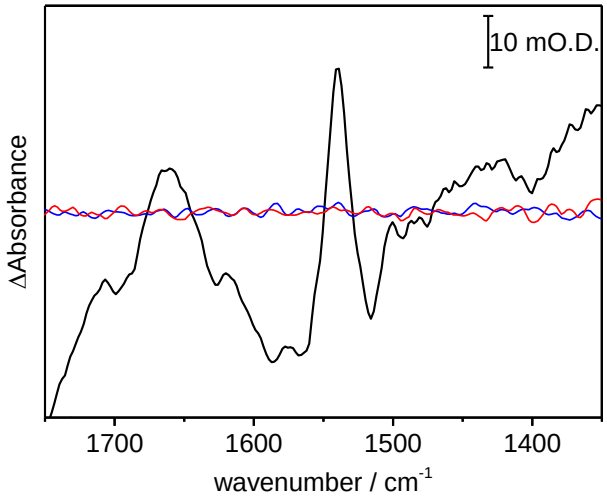


Spectroelectrochemistry of FMN adsorbed on carbon black particles. Oxidized *minus* reduced difference spectrum recorded in the microspectroscopy cell (black), reproduced from Figure 3 of the main text, compared to oxidized *minus* oxidized (red, calculated from the first and fourth oxidative potential steps at +0.242 V *versus* the standard hydrogen electrode) and reduced *minus* reduced (blue, calculated from the first and fourth reductive potential steps at -0.558 V *versus* the standard hydrogen electrode) difference spectra. The oxidized *minus* oxidized and reduced *minus* reduced difference spectra demonstrate the reproducibility and reversibility of the electrochemically-induced spectra recorded in the microspectroscopy cell, paving the way for future time-resolved measurements. These spectra also provide an indication of the baseline signal-to-noise ratio of the microspectroscopic approach, with a peak-to-peak noise level better than 1.5 mO.D. above 1450 $cm^{-1}$.

**Figure S6.** NuoF CE oxidized *minus* reduced difference spectrum compared to the baseline noise level.

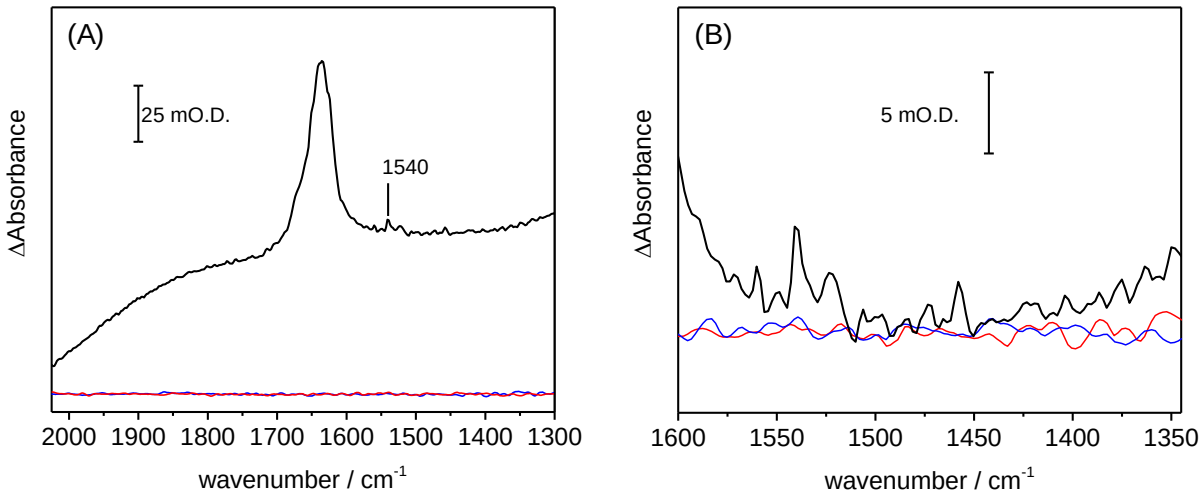


(A) Expanded view of the difference spectrum shown in Figure 4 of the main text, showing potential-induced changes in the H-O-H bend of water solvent around 1640 $cm^{-1}$. The absolute signal-to-noise level of the measurement in the region of the flavin bands (around 1540 $cm^{-1}$) can be judged relative to the 1800 – 2000 $cm^{-1}$ region, which is free of interfering absorbances from amide bands of NuoF CE, and also to the baseline signal-to-noise level shown in Figure S2 (the red and blue spectra correspond to oxidized *minus* oxidized and reduced *minus* reduced FMN, respectively). (B) Comparison of the baseline signal-to-noise level in the region of the flavin bands of adsorbed NuoF CE.

**Figure S7.** No detectable flavin signals are observed in spectroelectrochemical measurements on *E. coli* cell-free extracts deficient in NuoF.

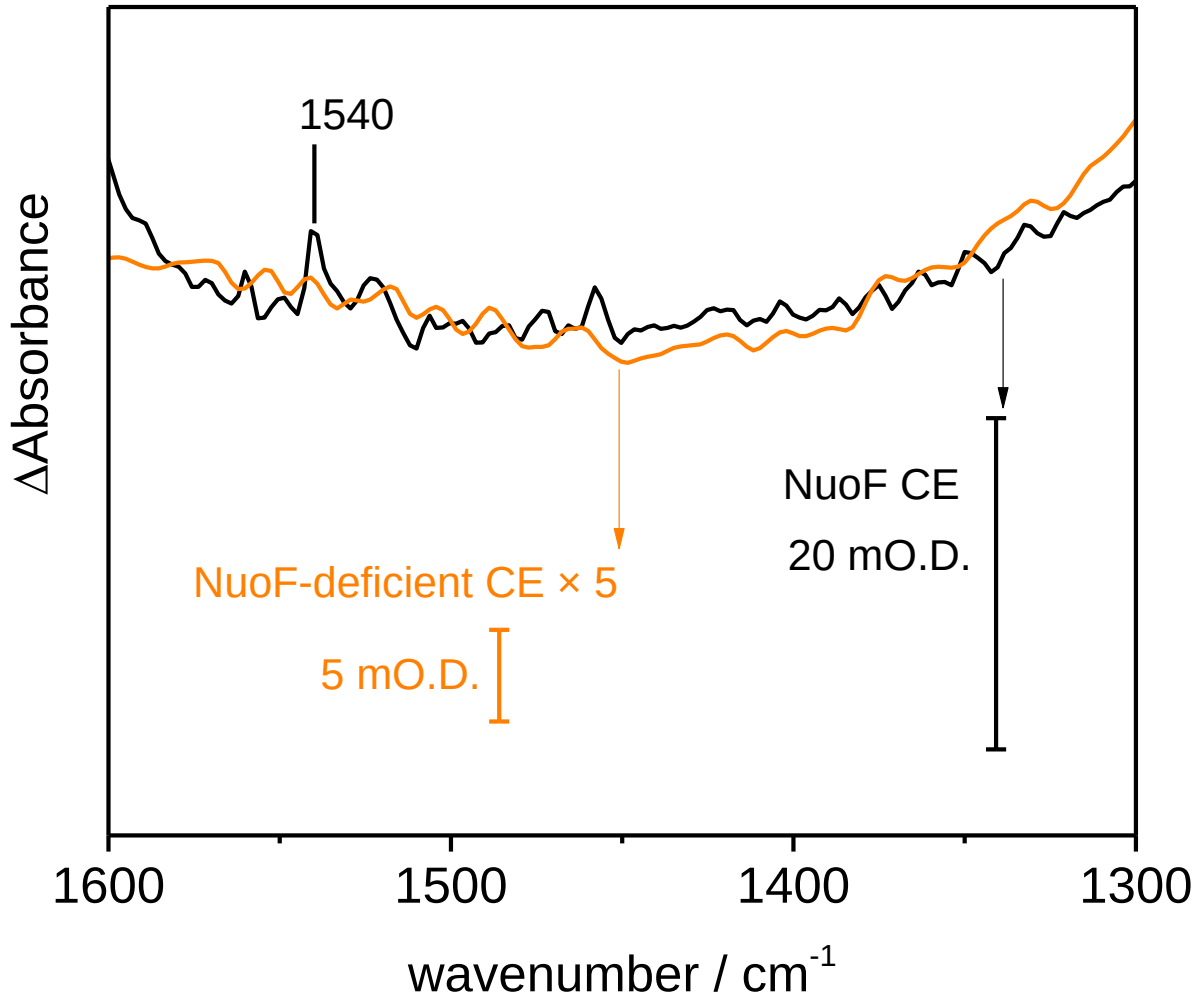


Oxidized *minus* reduced difference spectrum of NuoF CE (black, 20 mO.D. scale bar), as shown in Figure 4 of the main text, compared to an oxidized *minus* reduced difference spectrum of NuoF-deficient CE (orange, 5 mO.D. scale bar). No identifiable peaks due to either protein-associated or electrode-adsorbed FMN are observed in the NuoF-deficient CE sample, which has been multiplied by a factor of five to facilitate comparison.

**Figure S8.** *E. coli* Cell-free extract deficient in NuoF is inactive towards both $NAD^+$ reduction and NADH oxidation.

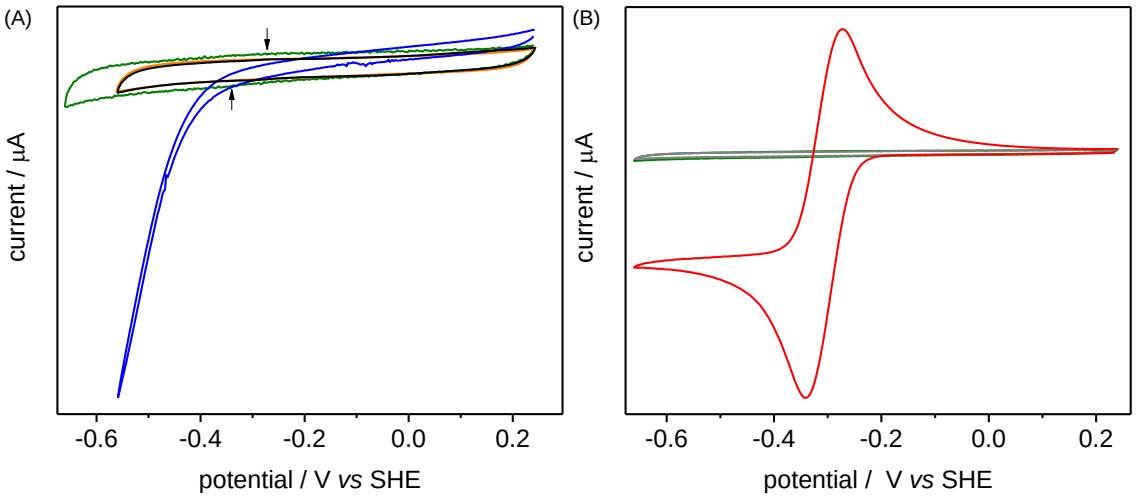


(A) Cyclic voltammograms recorded at a pyrolytic graphite 'edge' (PGE) rotating disc electrode modified with NuoF CE (dark blue), NuoF-deficient CE (orange) or FMN (green) immersed in potassium phosphate buffered electrolyte containing 1 mM $NAD^+$ and 1 mM NADH are shown against an unmodified electrode (black) under the same conditions. Only the electrode modified with NuoF CE shows electrocatalytic $NAD^+$/NADH interconversion. Small current peaks due to reduction and oxidation of electrode-immobilised FMN (green trace) are marked with arrows. (B) Cyclic voltammograms of an unmodified PGE electrode immersed in potassium phosphate buffered electrolyte (gray), after injection of 1 mM FMN in solution (red, no electrode rotation), and the same electrode immediately after exchanging the electrolyte for FMN-free buffer containing 1 mM $NAD^+$ and 1 mM NADH (green, reproduced from panel A and virtually indistinguishable from the unmodified electrode). No electrocatalytic $NAD^+$/NADH interconversion is observed, even over the wider potential range relative to the enzyme-modified electrodes. Experimental details: potentials were converted to V *vs* standard hydrogen electrode (SHE) using the conversion $E$(SHE)=$E$(SCE)+242 mV at 25°C; the electrode was rotated at 2000 rpm in all cases, apart from the solution FMN measurement in panel B.